

PAPER • OPEN ACCESS

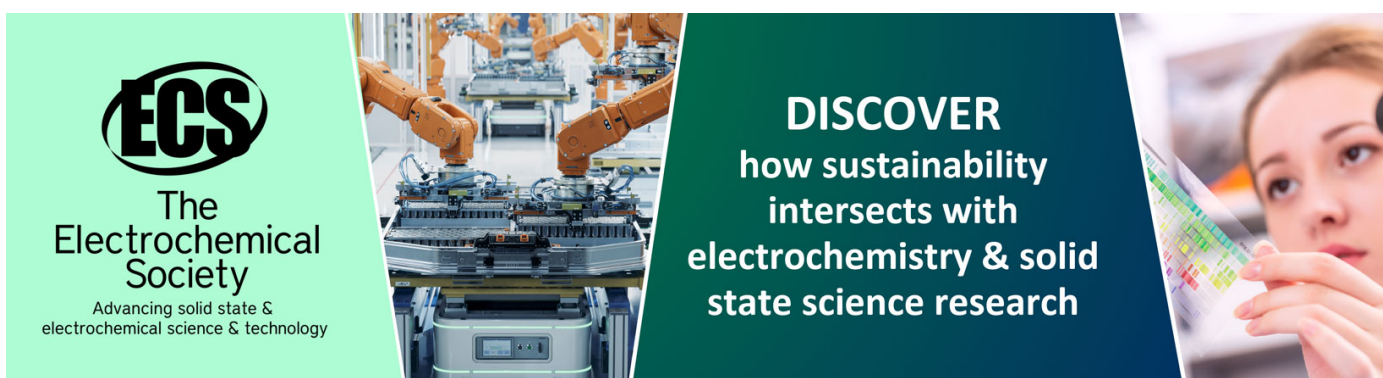
## Fluid-dynamic study of the behavior of the air inside a textile Stenter

To cite this article: J W Parra *et al* 2021 *J. Phys.: Conf. Ser.* **2118** 012006

View the [article online](#) for updates and enhancements.

You may also like

- [\(Research Award of the Electrodeposition Division\) Mathematical Modeling in Electrodeposition Studies](#)  
Alan West
- [Investigation of the influence of the angle of the installation of the blades of the impeller of the regenerative pump on its energy characteristics by the methods of hydrodynamic modeling](#)  
A Petrov, N Isaev and S Radchenko
- [Computer modeling of the parameters of the internal microclimate of buildings with green inserts inside](#)  
V I Telichenko, A A Benuzh and V V Fateeva



**ECS**  
The  
Electrochemical  
Society  
Advancing solid state &  
electrochemical science & technology

**DISCOVER**  
how sustainability  
intersects with  
electrochemistry & solid  
state science research

# Fluid-dynamic study of the behavior of the air inside a textile Stenter

J W Parra<sup>1</sup>, M B Quadri<sup>2</sup>, and D C Rodríguez<sup>1</sup>

<sup>1</sup> Grupo de Investigación en Química Básica Aplicada, Universidad Francisco de Paula Santander, San José de Cúcuta, Colombia

<sup>2</sup> Laboratório de Sistemas Porosos, Universidade Federal de Santa Catarina, Florianópolis, Brasil

E-mail: johnwilverpl@ufps.edu.co

**Abstract.** In the textile industry, drying is one of the most important processes. This process requires large investments and high energy consumption, which generates high costs for companies in this sector. In this work, a modeling of the behavior of the air was carried out in a textile Stenter, under real operating conditions through the development of fluid-dynamic simulations. For the computational modeling of the problem, a 3D geometry was constructed based on measurements taken from an injector of a textile Stenter. The standard k- $\epsilon$  turbulence model was used in the turbulent flow solution. The equations of the model were solved numerically using the finite element method. The standard k- $\epsilon$  turbulence model proved to be a model capable of reproducing the behavior of the air in the injectors of the textile Stenter.

## 1. Introduction

In the textile industry, drying is one of the most important processes. From a physical point of view, the drying of the fabric can be defined as a balance between the transfer of heat from the air stream to the surface of the fabric and the transfer of moisture from the surface of the fabric to the air stream. This process requires large investments and high energy consumption, which generates significant costs for companies in this sector. In industrialized countries, around 7% to 15% of the energy generated for industrial purposes is generally used for drying with relatively low thermal efficiency [1].

Therefore, it is of great interest to find ways to reduce energy demand without damaging the final characteristics of the fabric. Textile Stenters are thermal equipment used to dry fabrics in a continuous process. In the drying chambers, hot air flows over the fabric and dries it by convection with the exchange of heat and mass. The exhaust system removes the vapors resulting from the drying of the fabric, reducing the humidity of the air in the system and, consequently, increasing the drying efficiency in the process [2].

In the literature there are several studies on turbulent air jets, in which they carry out numerical studies, comparing different types of turbulence models with experimental values, this in order to study the heat and mass transfer applied in industrial processes, including drying. For example, Shi Y, *et al*, [3] studied the used of the standard turbulence model and the Reynolds stress model (RSM), model to calculate the heat transfer for a single semi-confined turbulent jet, which impinges on a flat plate, using different airflow parameters and different geometric parameters. For low heat flux values (1000 W/m<sup>2</sup> - 6000 W/m<sup>2</sup>), the physical properties of air were independent of



temperature and heat flux; however, for high heat flux (50000 W/m<sup>2</sup>), they observed that the physical properties of air were dependent on temperature.

Colucci and Viskanta [4] studied the effect of the geometry of a hyperbolic nozzle on local heat transfer coefficients, for this, they used a thermochromic liquid crystal technique to visualize and record isotherms on a uniformly heated impact surface. The authors concluded that the heat transfer coefficients at the site of incidence of the confined jets are more sensitive to the Reynolds number and the space between the nozzle and the plate, than the respective coefficients for the unconfined jets. Other authors who used the liquid crystal technique were Lee J. and Lee S [5]. They studied the effects of the nozzle outlet configuration on improvements in heat transfer, experimenting with three different types of nozzles.

Wang and Mujumdar [6] used 5 low Reynolds number models to study a two-dimensional turbulent jet, most of the models showed good agreement with the experimental data, both in the stagnant regions and in the jet walls. Gulati P, *et al* [7]. Studied the effects of the nozzle shape, the space between the plate and the jet, and Reynolds number, on the local heat transfer distribution of an air jet on a smooth and flat surface, for this they used three nozzles with different geometries: circular, square and rectangular, each with an equivalent diameter of 20 mm.

In this work the objective was to study the behavior of the air inside the drying chambers of a textile Stenter under real operating conditions, by obtaining speed fields, turbulent kinetic energy profiles and dissipation rate of turbulent air in the injectors, with in order to relate them to the phenomena of heat and mass transfer.

## 2. Materials and methods

This section presents the mathematical methodologies used to carry out the study this work.

### 2.1. Mathematical formulation

The simulations were carried out in COMSOL Multiphysics® version 4.4, a phenomenological simulation and modeling software. COMSOL Multiphysics® internally compiles the set of equations that represent the model in its entirety, generating a system of linear equations. The resolution of the model is obtained by the finite element method (FEM), which is numerical procedure used to solve systems of partial differential equations (PDE), and consists of dividing the domain of the solution into regions of simple form or by elements. Then, a rough solution for electronic data processing can be developed for each of these elements. The total solution is generated by joining the individual solutions and, at the same time, continuity at the boundaries between the elements is ensured [8]. For this study, the standard  $k$ - $\varepsilon$  turbulence model was used, which is the most used for computational simulations, since it presents good convergence and requires relatively few computational resources.

### 2.2. $k$ - $\varepsilon$ turbulence model

Turbulence is a phenomenon in which fluid particles mix in a non-linear way, which is described through various models of turbulence; the turbulence model ( $k$ - $\varepsilon$ ), used in this work is governed by two parameters:  $k$  related to the kinetic energy of the turbulence (defined as the variation of the fluctuations in speed) and  $\varepsilon$  the dissipation of the turbulence eddy (the rate at which speed fluctuations dissipate) [9]. Turbulent stresses are modeled through turbulent viscosity that include the parameters  $k$  and  $\varepsilon$ . For the steady state, the values of  $k$  and  $\varepsilon$  come directly from the differential equations for turbulence kinetic energy transport and the turbulence dissipation rate (see Equation (1) and Equation (2), respectively [10]).

$$\rho \mathbf{u} \cdot \nabla \mathbf{k} = \nabla \cdot \left( \left( \mu + \frac{\mu_T}{\sigma_k} \right) \nabla \mathbf{k} \right) + P_k - \rho \varepsilon, \quad (1)$$

$$\rho \mathbf{u} \cdot \nabla \varepsilon = \nabla \cdot \left( \left( \mu + \frac{\mu_T}{\sigma_\varepsilon} \right) \nabla \varepsilon \right) + C_{\varepsilon 1} \frac{\varepsilon}{k} P_k - C_{\varepsilon 2} \rho \frac{\varepsilon^2}{k}, \quad (2)$$

where  $\mathbf{u}$  is the velocity,  $\rho$  the density and  $\mu$  the viscosity of the fluid;  $C_{\varepsilon 1}$ ,  $C_{\varepsilon 2}$  and  $C_\mu$  are constants equal to 1.44, 1.92 and 0.09 respectively.  $\sigma_k = 1.0$  is the turbulent Prandtl number for  $k$  and  $\sigma_\varepsilon$  is the turbulent Prandtl number for  $\varepsilon$ . The Equation (3) calculate  $P_k$  is the turbulent kinetic energy production due to buoyancy and viscous forces [10].

$$P_k = \mu_T \left( \nabla \mathbf{u} : (\nabla \mathbf{u} + (\nabla \mathbf{u})^T) - \frac{2}{3} (\nabla \cdot \mathbf{u})^2 \right) - \frac{2}{3} \rho k \nabla \cdot \mathbf{u}, \quad (3)$$

The Equation (4) calculate Turbulent viscosity  $\mu_T$  is modeled by [10].

$$\mu_T = \rho C_\mu \frac{k^2}{\varepsilon}. \quad (4)$$

### 2.3. Simulation parameters

During the development of this work, a technical visit was made to a company in the textile sector that uses direct heating textile Stenters; on this visit, we were able to access the textile Stenter injectors (see Figure 1) and their measurements were also taken with a tape measure.



**Figure 1.** Photographs of the injector of a textile Stenter.

With the dimensions measured to the injectors during the technical visit, it was possible to build a geometry closer to the real one; thus, a 3D geometry was constructed consisting of two injectors (upper and lower) and a rectangular section volume in the middle of them, which represents the fabric in motion at a translation speed of the fabric ( $V_{\text{fabric}}$ ) of 0.4 m/s entering longitudinally in the dryer ( $x$ -axis), as shown in Figure 2 and at a temperature of 30 °C. The following physical properties were considered for the cotton fabric: density of 1500 kg/m<sup>3</sup>, specific heat of 1339.78 J/kg K and thermal conductivity of 0.029 W/(m K) values used by [11]. In this case, the air enters the injectors at a speed ( $V_{\text{air}}$ ) of 5.0 m/s and 180 °C of temperature, operating parameters used in industry [2,11]. The air injector is made up of a duct 2.82 m long, 0.31 m wide and 0.06 m high at one end and 0.19 m at the other (see Figure 2).

Each injector has 170 nozzles (distributed in 5 rows of 34, not paired laterally). The nozzles used in textile Stenters have a hemi-toroidal shell rim; the hemi-toroidal shell shape of the nozzle aims to distribute the jet of air more efficiently over the tissue surface. The nozzles have an inlet diameter ( $D_{\text{nozzle}}$ ) of 0.015 m and a height ( $A_{\text{nozzle}}$ ) of 0.005 m. The space between the injectors and the surface of the cotton fabric is ( $H$ ) is 0.07 m. To represent the cotton fabric, a flat plate of 2.65 m long, 0.31 m wide and 0.0015 m thick was constructed.

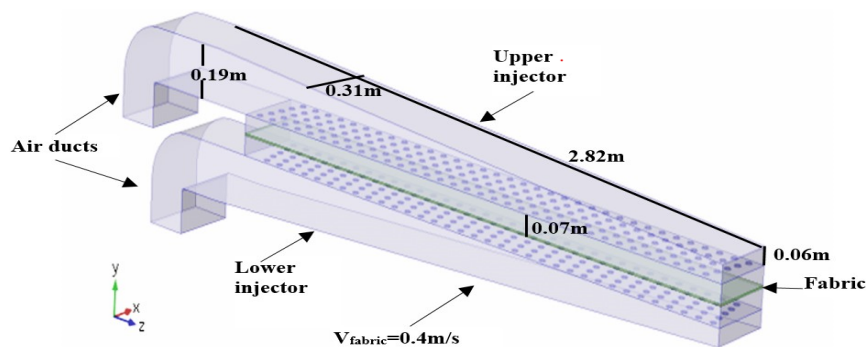


**Figure 2.** 3D geometry of the upper and lower injectors of a direct heating textile stenter.

#### 2.4. Geometry and discretization mesh

The construction of the mesh is one of the most important aspects to develop computational models, since the good construction of the mesh depends to a great extent on the convergence of a simulation, as well as the convergence time; due to the complexity of the domain, since it is composed of several subdomains, a mesh of eight hexahedral layers and 1018054 elements was built, which can be seen in Figure 3.

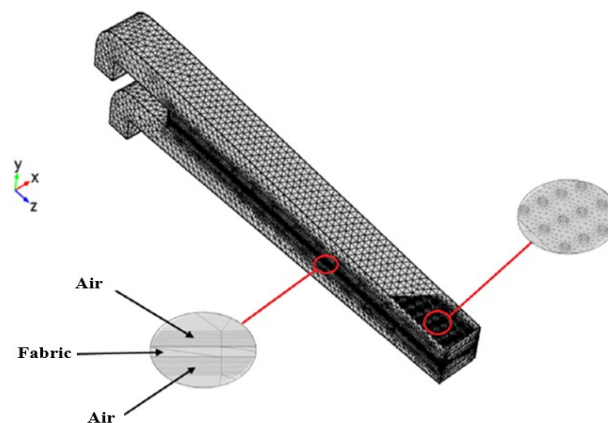


**Figure 3.** Generated mesh of a pair of injectors.

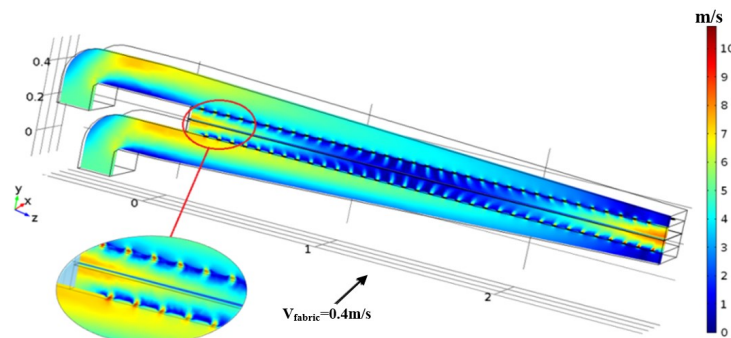
### 3. Results and discussions

The following is the analysis of the results obtained during the dynamic fluid study of the behavior of the air inside the textile Stenter used in the textile industry.

The objective to qualify and quantify the air flow in the region of the injectors of the dryer under study, by analyzing the velocity profiles, the streamlines and the turbulence parameters obtained from the  $k-\varepsilon$  turbulence model. As mentioned in section 2.3, velocities of 5.0 m/s were adopted for the air inlet velocity in the reference injectors and 0.4 m/s for the fabric displacement velocity.

In Figure 4, which shows the flow of air developed at steady state, it is possible to discern the velocity fields along a longitudinal section plane of the injectors, including the tissue surface. When analyzing the behavior of the air in the injector, it is observed that the highest velocity values are reached at the end nozzles where values between 8 m/s and 10 m/s are observed, showing that, in these areas of the injectors, the air reaches up to twice the inlet velocity. In the nozzles of the central region, the velocity reaches values between 4 m/s and 7 m/s.

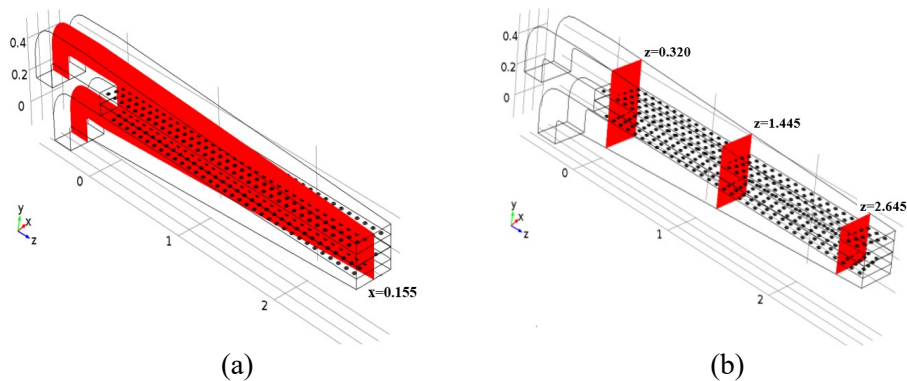
It can also be observed that, together with the extreme nozzles up to the surface of the tissue, the jets promote an intensification of the air velocity, inducing the appearance of vortices that characterize the behavior of the turbulent flow.



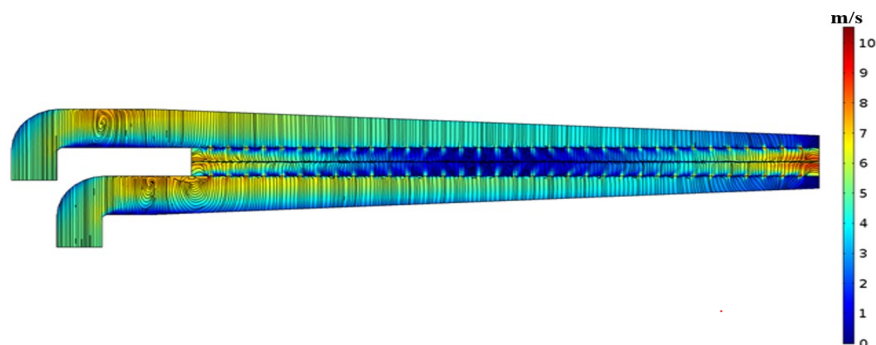
**Figure 4.** Velocity field in the injectors.

Figure 5, Figure 6 and Figure 7 present the flow velocity fields and streamlines in 2D graphs of longitudinal ( $z$ - $y$ ) and transverse ( $x$ - $y$ ) sections. Figure 5(a) corresponds to the injector cut in the ( $z$ - $y$ ) plane for  $x = 0.155$  and Figure 5(b) corresponds to the injector cut in the ( $x$ - $y$ ) plane for  $z = 0.320$ ,  $z = 1.445$  and  $z = 2.645$ .

The air recirculation areas near the inlet of the ducts that lead the air to the injectors are shown in Figure 6. Note that the velocity values in these regions are high; according to [12], this is due to the fact that recirculation restricts the passage of air freely, forming a stagnant region. Thus, due to the laws of conservation of mass and motion, the air accelerates in this region and moves towards the interior of the injector, subsequently losing speed.



**Figure 5.** Injector cuts (a) in the ( $z$ - $y$ ) plane and (b) in the ( $x$ - $y$ ) plane.



**Figure 6.** Velocity field and streamlines in the ( $z$ - $y$ ) plane with cutoff at  $x = 0.155$ .

In Figure 7 it can be seen that the current lines inside the injectors are quite orderly and uniform, as they leave them and meet the tissue, which is in motion, the lines begin to behave in a disorderly way and form vortices displaced in the direction of tissue movement.



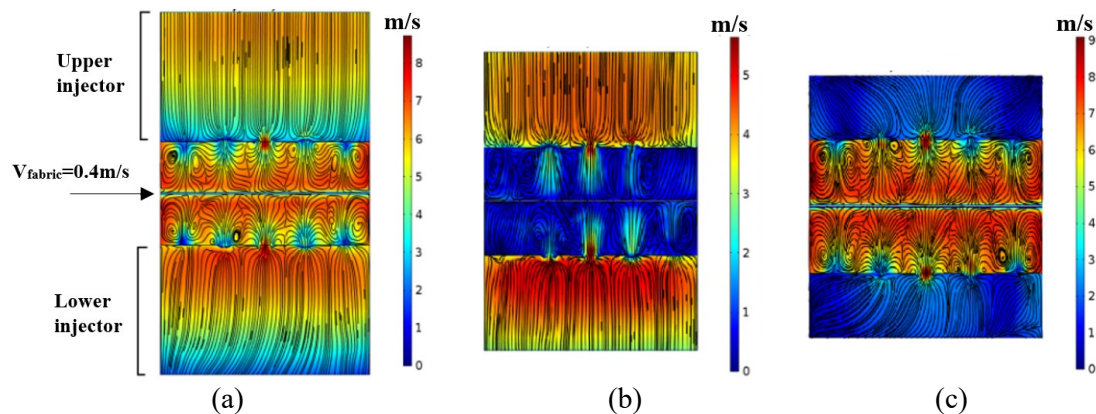


**Figure 7.** Field of velocities and streamlines in the (x-y) plane at (a)  $z = 0.32$ , (b)  $z = 1.445$ , and (c)  $z = 2.645$ .

In Figure 8, it can be seen that the turbulent kinetic energy has the highest values at the ends of the injectors; this is because the greatest flow accelerations occur in these regions. In the central region of the injectors, the turbulent kinetic energy tends to be lower.

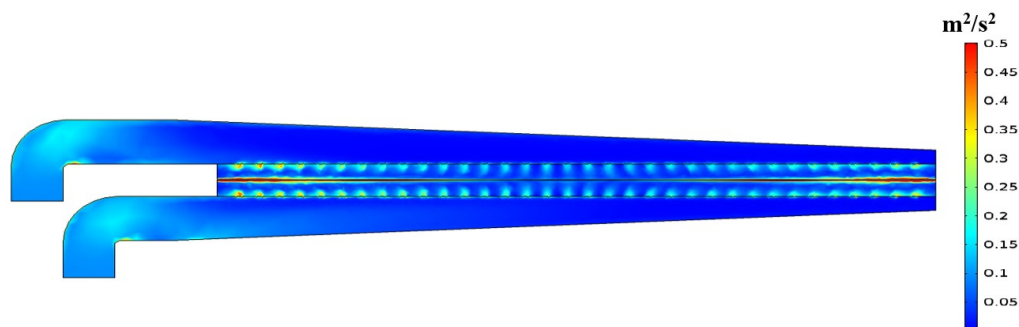


**Figure 8.** Turbulent kinetic energy in the (z-y) plane at  $x = 0.155$ .

The rate at which energy dissipates is shown in Figure 9. It is observed that the behavior is very similar to that of turbulent kinetic energy, that is, the highest values are found at the ends of the injectors and are lowest in the central region.

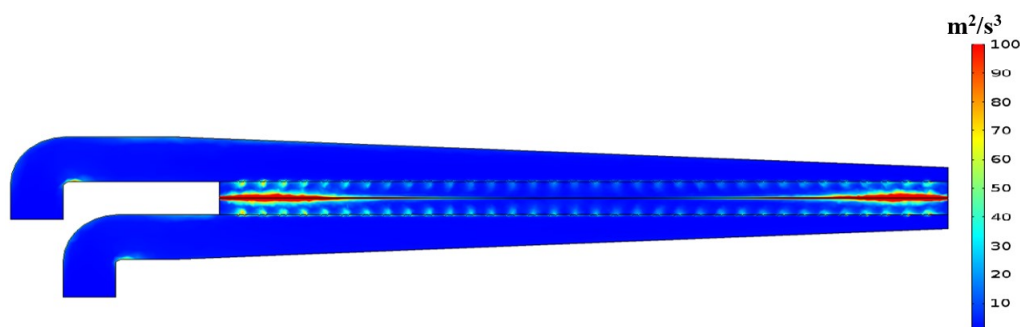


**Figure 9.** Turbulence dissipation rate in the (z-y) plane at  $x = 0.155$ .

A similar behavior was observed by Janzen J G, *et al* [13]. Who studied the turbulence properties of a viscous fluid through the oscillation of two grids; they observed the existence of two regions: a region close to the grids, where turbulence-producing effects are relevant (eventually also the advection resulting from the jets that form on the grids); and a second region (further from the gratings) in which there is a decrease in turbulent kinetic energy.

#### 4. Conclusions

Regarding the air flow patterns inside the textile Stenter, the  $k - \epsilon$  turbulence model allowed to consistently simulate the fluid-dynamic behavior of the air according to the operating conditions. By studying the behavior of the air in the injectors, the velocity profiles could be obtained, observing a non-uniform distribution of the intensity of the jets in the nozzles along them. The speed reached maximum values at the ends of the injectors. The formation of eddies and stagnant regions with behavior physically consistent with the fluid-dynamic principles applied to the geometry under study, was also evidenced. It is concluded, therefore, that the distribution of the air inside the dryer is not uniform for the geometry studied, which does not allow to support the statements, generally made by manufacturers of these equipment with geometries similar to the one studied, regarding the homogeneity of drying conditions.

#### References

- [1] Oktay Z, Hepbasli A 2002 Performance evaluation of a heat pump assisted mechanical opener dryer *Energy Conversion and Management* **44** 1193
- [2] Ferraz A D 2010 *Rio Oil & Gas Expo and Conference 2010* (Rio de Janeiro: Instituto Brasileiro de Petróleo, Gás e Biocombustíveis)
- [3] Shi Y, Ray M B, Mujumdar A S 2002 Computational study of impingement heat transfer under a turbulent slot jet *Ind. Eng. Chem. Res.* **41** 4643
- [4] Colucci D W, Viskanta R 1996 Effect of nozzle geometry on local convective heat transfer to a confined impinging air jet *Experimental Thermal and Fluid Science* **13** 71
- [5] Lee J, Lee S J 2000 The effect of nozzle configuration on stagnation region heat transfer enhancement of axisymmetric jet impingement *Int. J. Heat Mass Trans.* **43** 3497
- [6] Wang S J, Mujumdar A S 2005 A comparative study of five low Reynolds number  $k - \epsilon$  models for impingement heat transfer *Applied Thermal Engineering* **25** 31
- [7] Gulati P, Katti V, Prabhu S V 2008 Influence of the shape of the nozzle on local heat transfer distribution between smooth flat surface and impinging air jet *Int. J. of Ther. Scie.* **48** 602
- [8] Chapra S C, Canale R P 2008 *Métodos Numéricos para Ingenieros, 5ª edición* (Mexico: McGraw Hill)
- [9] Heuert J, Khatchatourian O 2007 *Congresso Nacional de Matemática Aplicada e Computacional* (Florianópolis: Sociedade Brasileira de Matemática Aplicada e Computacional)
- [10] Jones W P, Launder B E 1972 The prediction of laminarization with a two-equation model of turbulence *International Journal of Heat and Mass Transfer* **15** 301
- [11] Santos R M, Parra J W, Quadri M B, Rocha I C 2015 Study of drying and consumption of natural gas in a textile stenter of direct heating *Dry Technol.* **33** 37
- [12] Galarça M M 2004 *Análise Numérica para Modelos de Turbulência  $k - \omega$  E SST/  $k - \omega$  para O escoamento de Ar No Interior de Uma Lareira de Pequeno Porte. Modelagem Da Turbulência* (Porto Alegre: Universidade Federal do Rio Grande do Sul)
- [13] Arantes E J, Porto R M, Gulliver J S, Lima A, Schulz H E 2010 Lower nappe aeration in smooth channels: experimental data and numerical simulation *Anais da Academia Brasileira de Ciências* **82** 521